Therapeutic role of histone deacetylase inhibition in an *in vitro* model of Graves' orbitopathy

HYEONG JU BYEON[1], SOO HYUN CHOI[2], DON O. KIKKAWA[3], JAESANG KO[2] and JIN SOOK YOON[2]

[1]Department of Ophthalmology, Gangnam Severance Hospital, Yonsei University College of Medicine, Seoul 06273, Republic of Korea; [2]Department of Ophthalmology, Severance Hospital, Institute of Vision Research, Yonsei University College of Medicine, Seoul 03722, Republic of Korea; [3]Division of Oculofacial Plastic and Reconstructive Surgery, Department of Ophthalmology, Shiley Eye Institute, University of California San Diego, La Jolla, CA 92037, USA

Received March 2, 2024; Accepted August 20, 2024

DOI: 10.3892/mmr.2024.13342

Abstract. Graves' orbitopathy (GO), a manifestation of Graves' disease, is characterized by orbital fibroblast-induced inflammation, leading to fibrosis or adipogenesis. Histone deacetylase (HDAC) serves a central role in autoimmune diseases and fibrosis. The present study investigated HDAC inhibition in orbital fibroblasts from patients with GO to evaluate its potential as a therapeutic agent. Primary cultured orbital fibroblasts were treated with an HDAC inhibitor, panobinostat, under the stimulation of IL-1β, TGF-β or adipogenic medium. Inflammatory cytokines, and fibrosis- and adipogenesis-related proteins were analyzed using western blotting. The effects of panobinostat on HDAC mRNA expression were measured in GO orbital fibroblasts, and specific HDACs were inhibited using small interfering RNA transfection. Panobinostat significantly reduced the IL-1β-induced production of inflammatory cytokines and TGF-β-induced production of fibrosis-related proteins. It also suppressed adipocyte differentiation and adipogenic transcription factor production. Furthermore, it significantly attenuated HDAC7 mRNA expression in GO orbital fibroblasts. In addition, the silencing of HDAC7 led to anti-inflammatory and anti-fibrotic effects. In conclusion, by inhibiting HDAC7 gene expression, panobinostat may suppress the production of inflammatory cytokines, profibrotic proteins and adipogenesis in GO orbital fibroblasts. The present *in vitro* study suggested that HDAC7 could be a potential therapeutic target for inhibiting the inflammatory, adipogenic and fibrotic mechanisms of GO.

Correspondence to: Professor Jaesang Ko or Professor Jin Sook Yoon, Department of Ophthalmology, Severance Hospital, Institute of Vision Research, Yonsei University College of Medicine, 50-1 Yonsei-ro, Seodaemun, Seoul 03722, Republic of Korea
E-mail: jaesangko@yuhs.ac
E-mail: yoonjs@yuhs.ac

Key words: Graves' orbitopathy, orbital fibroblast, histone deacetylase inhibitor, histone deacetylase 7, panobinostat

Introduction

Graves' orbitopathy (GO) is a type of orbital inflammation that occurs in 15-30% of Graves' disease cases (1,2). GO clinically presents with eyelid retraction, exophthalmos and extraocular muscle enlargement; notably, 3-5% of patients experience a vision-threatening severe form, including compressive optic neuropathy and corneal exposure (2,3).

Dysregulated orbital fibroblasts and infiltration of orchestrated mononuclear cells, such as macrophage, T cells and B cells, are pivotal to the pathogenesis of GO. Autoantibodies targeting the thyrotropin and insulin-like growth factor 1 receptors initiate monocyte infiltration by T and B cells, as well as macrophages (4). These activated monocytes release cytokines that stimulate orbital fibroblasts, which also produce proinflammatory cytokines that exacerbate and maintain ocular inflammation (2,5). Stimulated orbital fibroblasts proliferate to produce glycosaminoglycans and differentiate into adipocytes or myofibroblasts, eventually leading to orbital tissue swelling, enlargement and fibrosis (2,4,5).

In a previous study on the pathogenesis and potential therapies for GO, no significant genotypic differences were found between patients with GO and without GO (6,7). Current research has focused on epigenetic and environmental factors (8,9), highlighting histone deacetylases (HDACs) as promising epigenetic molecules. HDACs are classified into four groups based on their enzymatic domain organization. Zn^{2+}-dependent HDACs, also known as classical HDACs, include Class I (HDACs 1, 2, 3 and 8), Class IIa (HDACs 4, 5, 7 and 9), Class IIb (HDACs 6 and 10) and Class IV (HDAC11), whereas Class III (sirtuins) molecules are NAD^+-dependent. HDACs mediate the deacetylation of lysine residues on the histone tail as a post-translational modification and inhibit transcription factor access to the DNA (10). This modification regulates gene transcription, controlling the cell cycle and immunological pathways (11). In addition to histone proteins, deacetylation occurs in several non-histone proteins, including transcription factors, and proteins involved in metabolism and the cell cycle (12). HDAC inhibitors (HDACis) have been approved by the US Food and Drug Administration to treat hematological tumors, such as cutaneous or peripheral T-cell lymphoma, and multiple myeloma, by inhibiting various

pathways involving cytokines, growth factors and protein kinases (13).

Although extensive research has been conducted on the role of HDACs in autoimmune diseases of the lungs and synovium (14-21), their role in GO pathogenesis remains largely unexplored (22). Among the HDACis that have been approved for hematological antitumor activity, panobinostat (LBH589), an orally available pan-HDACi, was approved by the US Food and Drug Administration in 2015 for the treatment of multiple myeloma (13). Panobinostat has ≥10-fold higher anticancer potency than vorinostat, another pan-HDACi, and its half-maximal inhibitory concentration values are lower than those of other pan-HDACis (23,24). Furthermore, panobinostat has been shown to exert superior anti-fibrotic effects on primary idiopathic pulmonary fibrosis compared with pirfenidone, the only currently available treatment for the condition (20).

The present study aimed to evaluate the effects of panobinostat on GO-induced inflammation, adipogenesis and fibrosis. Additional experiments were performed to assess which HDACs exert the therapeutic effects of panobinostat, with a particular focus on HDAC7.

Materials and methods

Tissue and cell preparation. During orbital surgery performed at Severance Hospital (Seoul, South Korea), orbital adipose tissue was collected from 10 patients with GO and 8 controls as a surgical byproduct (Table SI). The patients achieved euthyroid status with a clinical activity score (CAS) (25) <3 for ≥6 months, and the control individuals did not have GO or any other autoimmune diagnoses. The present study followed the tenets of The Declaration of Helsinki and was approved by the Institutional Review Board of Severance Hospital, Yonsei University College of Medicine (IRB no. 4-2022-0244; Seoul, South Korea). Written informed consent was obtained from all patients. Patient samples were collected between May 2022 and December 2023.

Orbital fat tissues were stored in RNAlater (Invitrogen; Thermo Fisher Scientific, Inc.) for RNA preparation. For primary cell culture, orbital fat was minced and cultured in Dulbecco's modified Eagle's medium/nutrient mixture F-12 (DMEM/F12; Welgene, Inc.) supplemented with 20% fetal bovine serum (FBS; Gibco; Thermo Fisher Scientific, Inc.) and 1% penicillin/streptomycin (Welgene, Inc.) in a humidified 5% CO_2 incubator at 37˚C. As orbital fibroblasts proliferated, the cells were serially passaged with trypsin/ethylenediaminetetraacetic acid. The cell strains were stored in liquid nitrogen (-196˚C). Cells between passages three and five were used for the subsequent experiments.

Peripheral blood mononuclear cell (PBMC) preparation. Peripheral venous blood (10 ml) from healthy donors (n=11) and patients with GO (n=32) was collected with ethics approval (IRB no. 4-2022-0244) (Table SII). Peripheral venous blood sampling was performed together with orbital tissue sampling. As peripheral venous blood was drawn prior to high-dose steroid therapy, the inclusion criteria were not restricted to CAS <3. Consequently, more samples were obtained from peripheral venous blood sampling than from orbital tissue samples. PBMC isolation was performed via Ficoll-Paque (Cytiva) density-gradient centrifugation at 1,000 x g for 20 min at 20˚C. PBMCs were preserved in TRIzol® (Invitrogen; Thermo Fisher Scientific, Inc.) at -80˚C in a freezer.

Cell viability assay. Orbital fibroblasts were seeded into 24-well culture plates ($1x10^5$ cells/well) and exposed to various concentrations of panobinostat (Selleck Chemicals) (untreated control, 10, 30, 50, 70 and 100 nM) for 24 h at 37˚C. Subsequently, the cells were washed and incubated with MTT solution (MilliporeSigma) for 2 h at 37˚C. After solubilization with dimethyl sulfoxide (MilliporeSigma), the dye absorbance was measured using a microplate reader (BioTek Instruments; Agilent Technologies, Inc.) at 560 and 630 nm. Cell viability was expressed as a percentage of the untreated control cells.

Reverse transcription-quantitative PCR (RT-qPCR). Orbital fat tissues were homogenized using a tissue homogenizer (Precellys 24; Bertin Instruments) and were lysed with TRIzol® (Invitrogen; Thermo Fisher Scientific, Inc.) using a Precellys lysing kit (hard tissue homogenizing CK28; cat. no. P000911-LYSK0-A; Bertin Instruments). RNA was also extracted from primary cultured GO orbital fibroblasts cultured with or without panobinostat (100 nM) for 24 h using TRIzol. The RNA concentration was measured using a NanoDrop spectrophotometer (Thermo Fisher Scientific, Inc.). cDNA was synthesized using a SensiFAST cDNA Synthesis Kit (Meridian Bioscience, Inc.) according to the manufacturer's protocol. qPCR amplification was performed using a QuantStudio3 real-time PCR thermocycler (Applied Biosystems; Thermo Fisher Scientific, Inc.) with specific primers and SYBR green PCR master mix (Takara Bio, Inc.). The thermocycling conditions were as follows: Activation at 50˚C for 2 min and incubation at 95˚C for 10 min, followed by 40 cycles of denaturation at 95˚C for 15 sec and annealing at 60˚C for 1 min, and a final melting curve analysis at 95˚C for 15 sec, 60˚C for 15 sec and 95˚C for 15 sec. The sequences of primers targeting multiple HDAC genes (class I: HDAC1, 2 and 3; class IIa: HDAC4, 5 and 7; class IIb: HDAC6 and 10) are detailed in Table SIII. The results were normalized to GAPDH and are displayed as fold change in cycle quantification (Cq) value relative to that of the controls, using the $2^{-\Delta\Delta Cq}$ method (26).

Western blotting. Orbital fibroblasts were treated with reagents, such as recombinant IL-1β (10 ng/ml), TGF-β (5 ng/ml) (both from R&D Systems, Inc.) and panobinostat (100 nM), for various durations in a humidified 5% CO_2 incubator at 37˚C. The cells were then washed with DPBS (Welgene, Inc.) and lysed using RIPA lysis buffer (Welgene, Inc.) containing a Halt™ Protease Inhibitor Cocktail (Thermo Fisher Scientific, Inc.). Protein concentrations were determined using the BCA assay (Pierce™ BCA Protein Assay Kit; cat. no. 23227, Thermo Fisher Scientific, Inc.). Proteins were boiled in sample buffer and equal amounts of protein (30 μg) were then resolved by SDS-PAGE on 8-15% gels, and were transferred to nitrocellulose membranes (MilliporeSigma). Subsequently, the membranes were incubated with 5% skim milk blocking buffer for 1 h at room temperature (25˚C). After overnight incubation with primary antibodies at 4˚C

(Table SIV), the bands were incubated with a secondary antibody [Pierce Goat Anti-Rabbit, (H+L), Peroxidase Conjugated (1:5,000; cat. no. 31460; Thermo Fisher Scientific, Inc.) and Pierce Goat Anti-Mouse, (H+L), Peroxidase Conjugated (1:5,000; cat. no. 31430; Thermo Fisher Scientific, Inc)] for 1 h at room temperature, after which, visualization was performed using SuperSignal™ West Pico PLUS chemiluminescent substrates (cat. no. 34580; Thermo Fisher Scientific, Inc.). Band intensities, measured using ImageJ software ver. 1.54 g (National Institutes of Health), were standardized to β-actin in the same sample.

Adipogenesis. Orbital fibroblasts were differentiated into adipocytes for 14 days using adipogenic solution as previously described (27). Briefly, the adipogenic solution consisted of DMEM (Welgene, Inc.) supplemented with 10% FBS (Thermo Fisher Scientific, Inc.), 33 μM biotin (Roche Diagnostics GmbH), 17 μM pantothenic acid (Roche Diagnostics GmbH), 10 μg/ml transferrin (Roche Diagnostics GmbH), 0.2 nM T3 (Roche Diagnostics GmbH), 1 μM insulin (Roche Diagnostics GmbH), 0.2 μM carbaprostaglandin (Calbiochem; Merck KGaA) and 10 μM rosiglitazone (Cayman Chemical Company), and the medium was replaced every 2-3 days. For the first 4 days, 10 μM dexamethasone (MilliporeSigma) and 0.1 mM isobutylmethylxanthine (MilliporeSigma) were added to induce adipogenesis. Cells were co-treated with panobinostat (10 nM) and/or IL-1β (10 ng/ml) for 14 days.

Oil Red O staining. Differentiated adipocytes treated with panobinostat (10 nM) and/or IL-1β (10 ng/ml) for 14 days of adipogenesis were washed with PBS, fixed with 10% formalin for 1 h at 4˚C and stained for 2 h at room temperature with Oil Red O (cat. no. O1516; MilliporeSigma) working solution (Oil Red O:deionized water=6:4, filtered). The plates were rinsed with PBS and the cells were observed under an inverted light microscope (IX73; Olympus Corporation) equipped with a charge-coupled device camera (DP71; Olympus Corporation). Oil Red O stain was solubilized with 100% isopropanol to quantify lipid accumulation, and the optical density was measured using a spectrophotometer at 490 nm.

Silencing of HDACs. Small interfering (si)RNAs targeting HDAC6 and HDAC7 (si-HDAC6 and si-HDAC7) were obtained from Dharmacon Reagents; Revvity, Inc. (SMARTpool format; cat. nos. L-003499-00 and L-009330-00), and a non-targeting negative control No. 1 siRNA (si-con) was obtained from Invitrogen; Thermo Fisher Scientific, Inc. (Table SV). siRNAs (10 nM) were transfected into 80% confluent orbital fibroblasts using Lipofectamine® RNAiMAX (Invitrogen; Thermo Fisher Scientific, Inc.). After 24 h in a humidified 5% CO_2 incubator at 37˚C, the medium was replaced with fresh complete medium containing 10% fetal bovine serum and antibiotics, and the cells were incubated for a further 48 h.

Statistical analysis. IBM SPSS Statistics for Windows v 29.0 (IBM Corp.) was used for statistical analysis. All experiments were performed twice using cells from 3 different patients. The results were averaged and expressed as the mean ± SD. Normal distribution was verified using the Kolmogorov-Smirnov test. For comparisons between the experimental and control groups, either unpaired Student's t-test or Mann-Whitney U-test was used. When comparing multiple groups, Kruskal-Wallis test was used, followed by Dunn's post hoc test. In the demographic analysis, Fisher's exact test was used to compare two categorical variables. $P<0.05$ was considered to indicate a statistically significant difference.

Results

mRNA expression levels of HDACs in orbital tissue and PBMC. Basal levels of HDAC transcripts were analyzed using RT-qPCR. A total of eight HDAC genes were assessed: Class I (HDAC1, 2 and 3), class IIa (HDAC4, 5 and 7) and class IIb (HDAC6 and 10). The median mRNA expression levels of HDAC3, 4, 5, 6 and 7 were significantly lower in orbital tissues from patients with GO (n=10) than in those from the control individuals (n=8) (Fig. 1). In addition, HDAC gene expression patterns were detected in the PBMCs of patients with GO (n=32) and normal controls (n=11). There were no significant differences in the mRNA expression levels of HDACs between patients with GO and normal controls (Fig. S1).

Effect of panobinostat on cell viability. An MTT assay was performed to determine the non-toxic concentration of panobinostat. In both normal and GO orbital fibroblasts, panobinostat at concentrations between 10 and 100 nM did not reduce cell viability to <95% over the course of a 24-h treatment (Fig. 2).

Suppression of HDACs by panobinostat in GO orbital fibroblasts. Even with panobinostat, a non-selective HDACi, not all HDAC genes were uniformly inhibited. Pan-HDACis can have different effects on each HDAC depending on the cellular context (28). To verify the selectivity of panobinostat for GO orbital fibroblasts, the fibroblasts were incubated for 24 h with and without panobinostat (100 nM), and the expression levels of various HDAC transcripts were analyzed using RT-qPCR. HDAC3 mRNA expression was found to be upregulated, whereas HDAC6 and HDAC7 mRNA levels were significantly downregulated in response to panobinostat (Fig. 3).

Therapeutic effect of panobinostat on stimulated orbital fibroblasts. The present study evaluated the therapeutic effects of panobinostat on multiple GO-related pathogenic processes (inflammation, adipogenesis and fibrosis) in primary cultured orbital fibroblasts. GO and normal orbital fibroblasts were pretreated with panobinostat (100 nM) for 30 min, followed by inflammatory stimulation using IL-1β (10 ng/ml) for 24 h. Western blotting demonstrated that panobinostat treatment suppressed the IL-1β-induced expression of the proinflammatory cytokines IL-6 and IL-8 (Fig. 4).

The stimulus was changed to TGF-β (5 ng/ml) under the same experimental conditions to investigate the anti-fibrotic effects of panobinostat. The increase in expression of the profibrotic cytokines fibronectin, collagen Iα and collagen 3 induced by TGF-β was significantly attenuated after panobinostat treatment (Fig. 5).

Finally, the effect of panobinostat on the adipocyte differentiation of orbital fibroblasts was examined. During the 14 days of adipogenesis in an adipogenic medium,

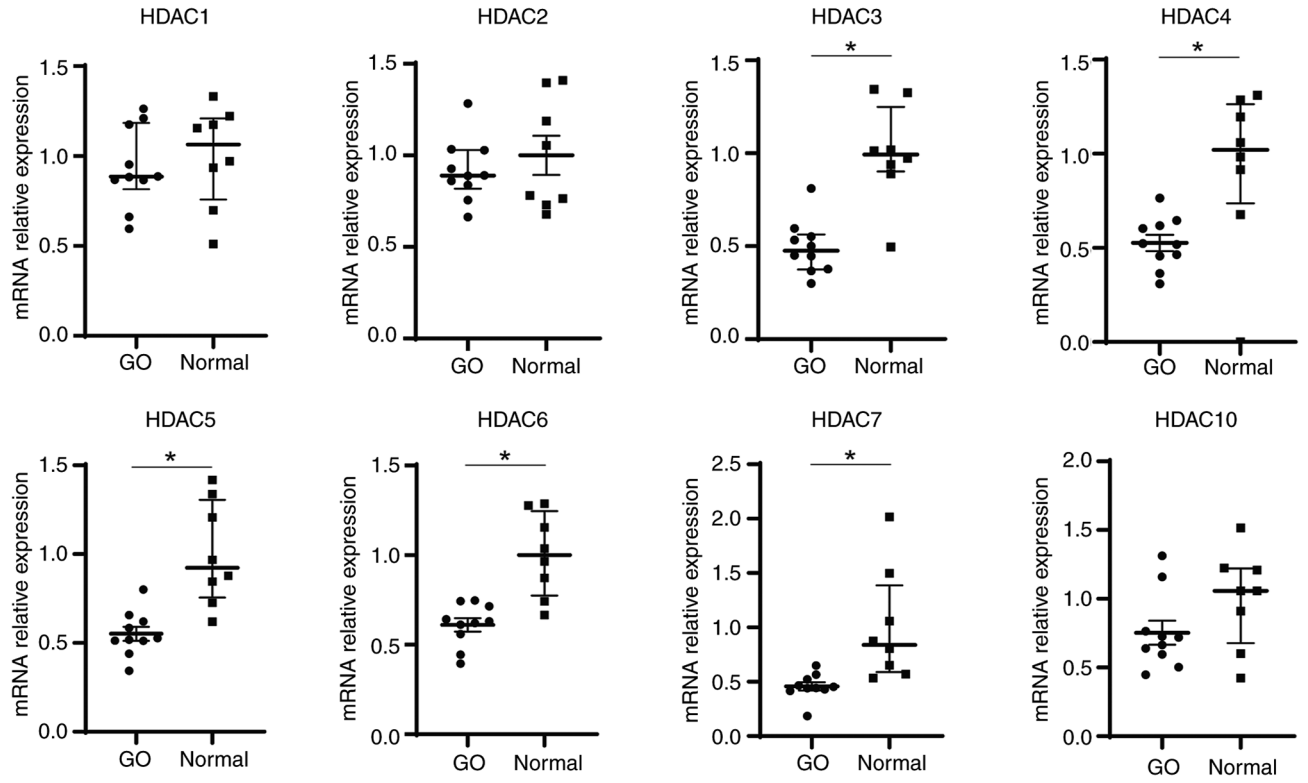

Figure 1. HDAC mRNA expression in GO and control orbital tissues. Orbital tissues from patients with GO (n=10) and controls (n=8) were analyzed to evaluate the mRNA expression levels of HDACs (class I: HDAC1, 2 and 3; class IIa: HDAC4, 5 and 7; class IIb: HDAC6 and 10). Reverse transcription-quantitative PCR was performed, and the results are presented as the median and interquartile ranges compared with normal controls. Statistical significance was determined using Mann-Whitney U-test. *P<0.05 vs. normal control. GO, Graves' orbitopathy; HDAC, histone deacetylase.

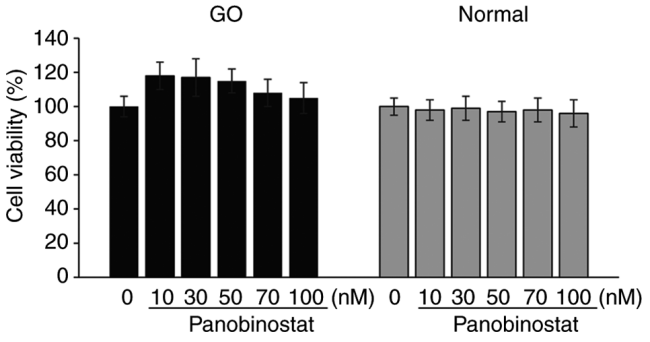

Figure 2. Cell viability after treatment with panobinostat. Orbital fibroblasts from patients with GO (n=3) and controls (n=3) were seeded in 24-well culture plates and treated with various concentrations of panobinostat (control, 10, 30, 50, 70 and 100 nM) for 24 h. The MTT assay was repeated twice for cells from 3 different individuals. Results are presented as the mean ± SD relative to the untreated control. GO, Graves' orbitopathy.

GO orbital fibroblasts were also co-treated with panobinostat (10 nM) and/or IL-1β (10 ng/ml). Panobinostat significantly mitigated IL-1β-induced adipogenesis (Fig. 6A), as demonstrated by the spectrophotometric lipid quantification (Fig. 6B). The expression levels of adiponectin, leptin, HDAC7 and all the investigated adipogenic transcription factors, including peroxisome proliferator-activated receptor γ, CCAAT-enhancer-binding protein (c/EBP)α, c/EBPβ and aP2, were reduced with panobinostat treatment compared with in cells under adipogenic differentiation and IL-1β stimulation (Fig. 6C and D).

Effect of panobinostat on signaling pathway molecules. The present study further investigated the intracellular signaling pathway molecules affected by panobinostat treatment. Orbital fibroblasts pretreated with panobinostat (100 nM) for 24 h were incubated with IL-1β (10 ng/ml) for 15 min. IL-1β-induced JNK and Akt phosphorylation was significantly reduced by panobinostat treatment in GO orbital fibroblasts, but not in normal cells (Fig. 7).

As major transducers of TGF-β, the SMAD pathway molecules SMAD1/5/9, SMAD2 and SMAD3 were investigated to determine the effect of panobinostat. Treatment with 100 nM panobinostat for 3 h significantly reduced TGF-β (5 ng/ml; 1 h)-induced SMAD3 phosphorylation in normal orbital fibroblasts, whereas this reduction was not significant in GO orbital fibroblasts (Fig. 8A). As non-SMAD pathway molecules, Akt, JNK, p38 and ERK expression levels were examined under TGF-β stimulation (5 ng/ml; 1 h) after panobinostat (100 nM) exposure for 3 h. Phosphorylation of Akt was attenuated in both GO and normal cells, whereas phosphorylation of p38 was reduced in normal cells (Fig. 8B).

Role of HDAC7 in GO orbital fibroblasts. Based on the results showing that HDAC7 was notably suppressed by panobinostat (Fig. 3), the effects of HDAC7 on GO orbital fibroblasts were examined. Similar to the results showing significantly lower HDAC mRNA levels in GO tissues than in normal tissues (Fig. 1), western blot analysis revealed that HDAC7 protein levels were also lower in GO tissues (n=7) than in normal tissues (n=7) (Fig. S2). GO orbital fibroblasts were then treated

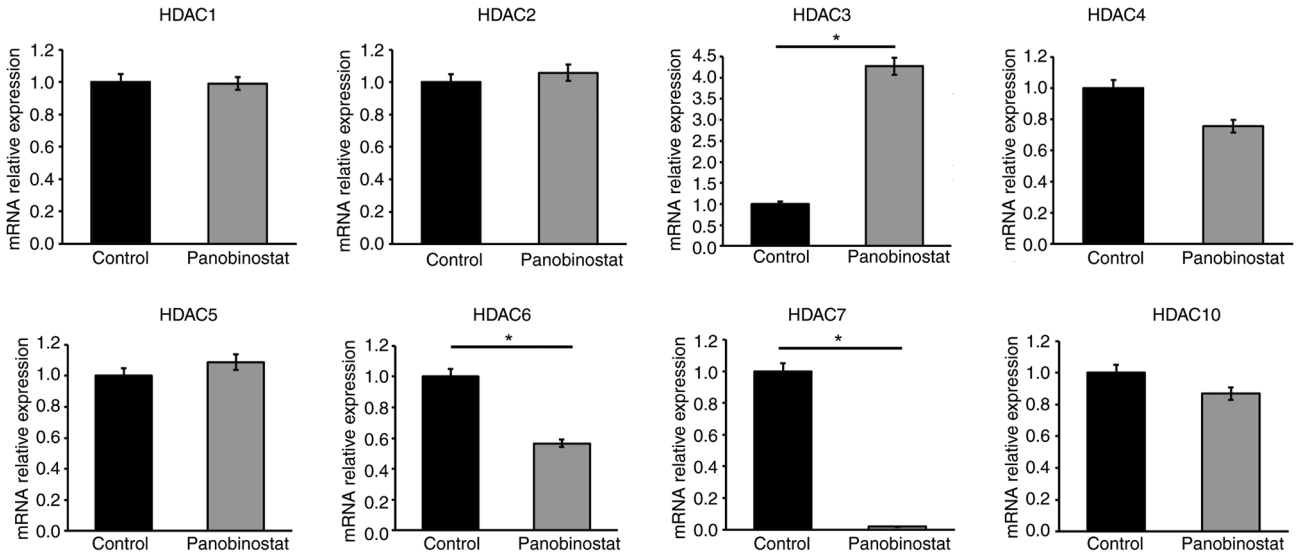

Figure 3. Effect of panobinostat on the mRNA expression levels of HDACs. Orbital fibroblasts from patients with GO (n=3) were cultured with panobinostat (100 nM) for 24 h. GO orbital fibroblasts cultured without panobinostat for 24 h were used as controls. mRNA expression levels of HDACs (class I: HDAC1, 2 and 3; class IIa: HDAC4, 5 and 7; class IIb: HDAC6 and 10) were measured by reverse transcription-quantitative PCR. All experiments were conducted twice on samples from 3 individuals. Results are presented as the mean ± SD relative to the control. Statistical significance was determined using Mann-Whitney U-test. *P<0.05 vs. untreated control. GO, Graves' orbitopathy; HDAC, histone deacetylase.

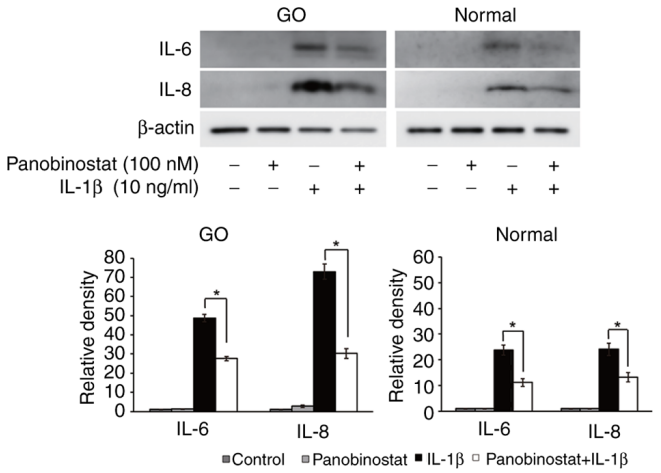

Figure 4. Suppressive effect of panobinostat on proinflammatory cytokine expression. Orbital fibroblasts from patients with GO (n=3) and controls (n=3) were pretreated with panobinostat (100 nM) for 30 min and then stimulated with IL-1β (10 ng/ml) for 24 h. Western blotting was performed to examine the protein expression levels of the proinflammatory cytokines IL-6 and IL-8. Representative gel images are shown. Densitometry was performed and levels were normalized to β-actin in the same sample. All experiments were conducted twice on samples from three individuals. Data are presented as the mean ± SD. Statistical significance was determined using Mann-Whitney U-test to compare the effect of panobinostat under IL-1β stimulation. *P<0.05. GO, Graves' orbitopathy.

with IL-1β (10 ng/ml) and TGF-β (5 ng/ml) for 0, 5, 10, 30 and 60 min. Western blot analysis revealed that HDAC7 protein levels were increased after 30 min of IL-1β stimulation and after 60 min of TGF-β stimulation (Fig. 9).

To elucidate the role of HDAC7, HDAC7 was silenced using siRNA (Fig. 10A). si-HDAC7 and si-con were transfected into cells for 24 h, which were then stimulated with IL-1β (10 ng/ml) or TGF-β (5 ng/ml) for 24 h to evaluate the effects on inflammation and fibrosis. IL-6 levels, which were increased following IL-1β treatment, were significantly reduced in both GO and normal orbital fibroblasts transfected with si-HDAC7, whereas IL-8 levels were only reduced in si-HDAC7-transfected normal orbital fibroblasts (Fig. 10B). HDAC7 silencing also significantly reduced the expression levels of the TGF-β-induced profibrotic proteins fibronectin and α-smooth muscle actin (α-SMA) in both GO and normal orbital fibroblasts, as well as collagen Iα and collagen 3 in GO cells (Fig. 10C).

Additional experiments were performed to determine the effects of HDAC3 and HDAC6, which were significantly upregulated and downregulated by panobinostat, respectively (Fig. 3). Firstly, HDAC6 was knocked down by siRNA transfection (Fig. S3A), and the orbital fibroblasts were treated with IL-1β (10 ng/ml) or TGF-β (5 ng/ml). The protein expression levels of the IL-1β-induced proinflammatory cytokines, IL-6 and IL-8, did not differ between cells transfected with si-HDAC6 and si-con (Fig. S3B). Upon TGF-β stimulation, the expression levels of profibrotic proteins, fibronectin and α-SMA, were downregulated by si-HDAC6 transfection in normal cells; however, the expression levels of Col1α and Col3 in normal cells and of all profibrotic proteins in GO cells showed no difference in response to si-HDAC6 transfection (Fig. S3C).

Secondly, as shown in Fig. 3, HDAC7 mRNA expression was decreased, whereas HDAC3 mRNA expression was significantly upregulated by panobinostat treatment. As the enzymatic activity of HDAC7 in the nucleus is influenced by HDAC3 (29), the effect of siHDAC7 on HDAC3 expression was investigated. The effects of panobinostat on the protein expression levels of HDAC3 and HDAC7 in orbital fibroblasts were confirmed by western blotting, demonstrating downregulation of HDAC7 and upregulation of HDAC3, in accordance with the mRNA results (Fig. S4A). However, silencing of HDAC7 did not affect the protein expression levels of HDAC3 in orbital fibroblasts (Fig. S4B).

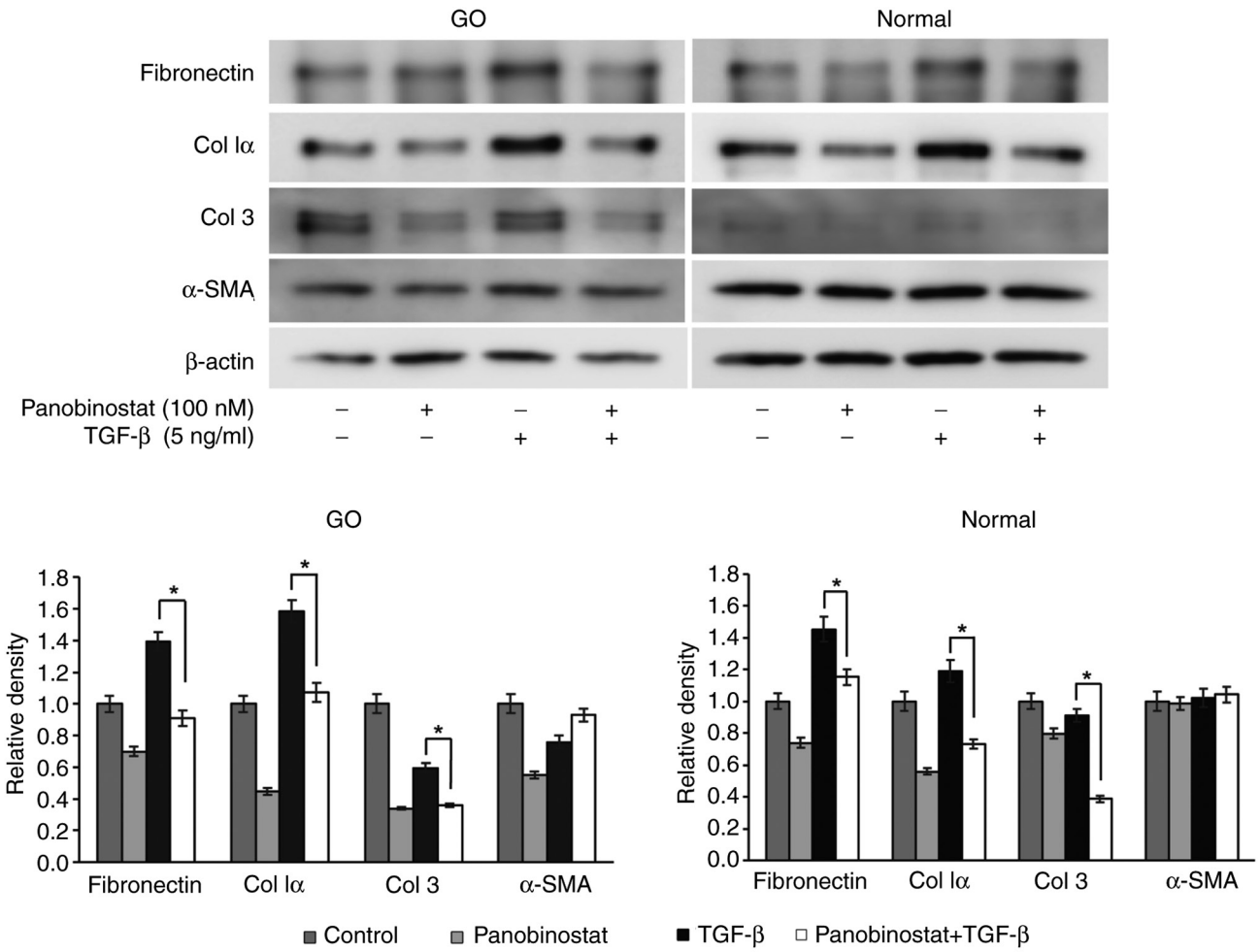

Figure 5. Suppressive effect of panobinostat on the expression of TGF-β-induced profibrotic proteins. Orbital fibroblasts from patients with GO (n=3) and controls (n=3) were pretreated with panobinostat (100 nM) for 30 min and then stimulated with TGF-β (5 ng/ml) for 24 h. The expression levels of the profibrotic proteins fibronectin, Col Iα, Col 3 and α-SMA were determined by western blot analysis. Representative gel images are shown. β-actin was used for normalization. All experiments were conducted twice on samples from three individuals. Data are presented as the mean ± SD. Statistical significance was determined using Mann-Whitney U-test to compare the effect of panobinostat under TGF-β stimulation. *P<0.05. α-SMA, α-smooth muscle actin; Col, collagen; GO, Graves' orbitopathy.

Discussion

In the present study, the pan-HDACi panobinostat was identified as a potent attenuator of orbital fibroblast activation. Panobinostat suppressed the expression of proinflammatory, profibrotic and adipogenic proteins induced by specific stimulators in orbital fibroblasts. Furthermore, it selectively inhibited different HDAC genes in GO orbital fibroblasts. Notably, blockage of HDAC7 was revealed to be associated with the therapeutic effect of panobinostat on GO pathogenesis.

The orbital tissues analyzed were primarily derived from patients undergoing orbital decompression surgery, typically performed during the inactive phase of GO. Most HDAC genes in GO orbital tissues exhibited reduced mRNA expression compared with that in normal orbital tissues, possibly due to negative feedback after the active phase. Additionally, HDAC7 protein expression was increased in orbital fibroblasts following stimulation with IL-1β and TGF-β. However, the present study revealed no significant differences in the mRNA expression levels of HDAC genes in PBMCs between patients with GO and healthy controls. This is in contrast to a previous study that reported elevated mRNA expression levels of HDAC1 and HDAC2 in PBMCs from patients with Graves' disease, leading to histone H4 hypoacetylation (30). This discrepancy could be because PBMCs are a mixed collection of different cells, such as T cells, B cells, macrophages and mast cells, which might obscure specific changes in HDAC expression. Furthermore, a number of systemic inflammatory diseases, such as rheumatoid arthritis and chronic obstructive pulmonary disease, can influence HDAC mRNA expression in PBMCs (31,32), while GO may represent a more localized inflammatory manifestation in the orbit. Therefore, despite the lack of differences in PBMC HDAC mRNA expression, HDACs may serve as specific biomarkers for tissue and localized therapeutic targets in GO pathogenesis, as the present study identified marked differences in HDAC expression in GO orbital tissue, and HDAC inhibition in orbital fibroblasts suppressed the expression of pro-inflammatory, adipogenic and pro-fibrotic proteins.

A recent report showed that HDAC4 expression was increased upon stimulation with platelet-derived growth factor-BB (PDGF-BB) in GO orbital fibroblasts, whereas

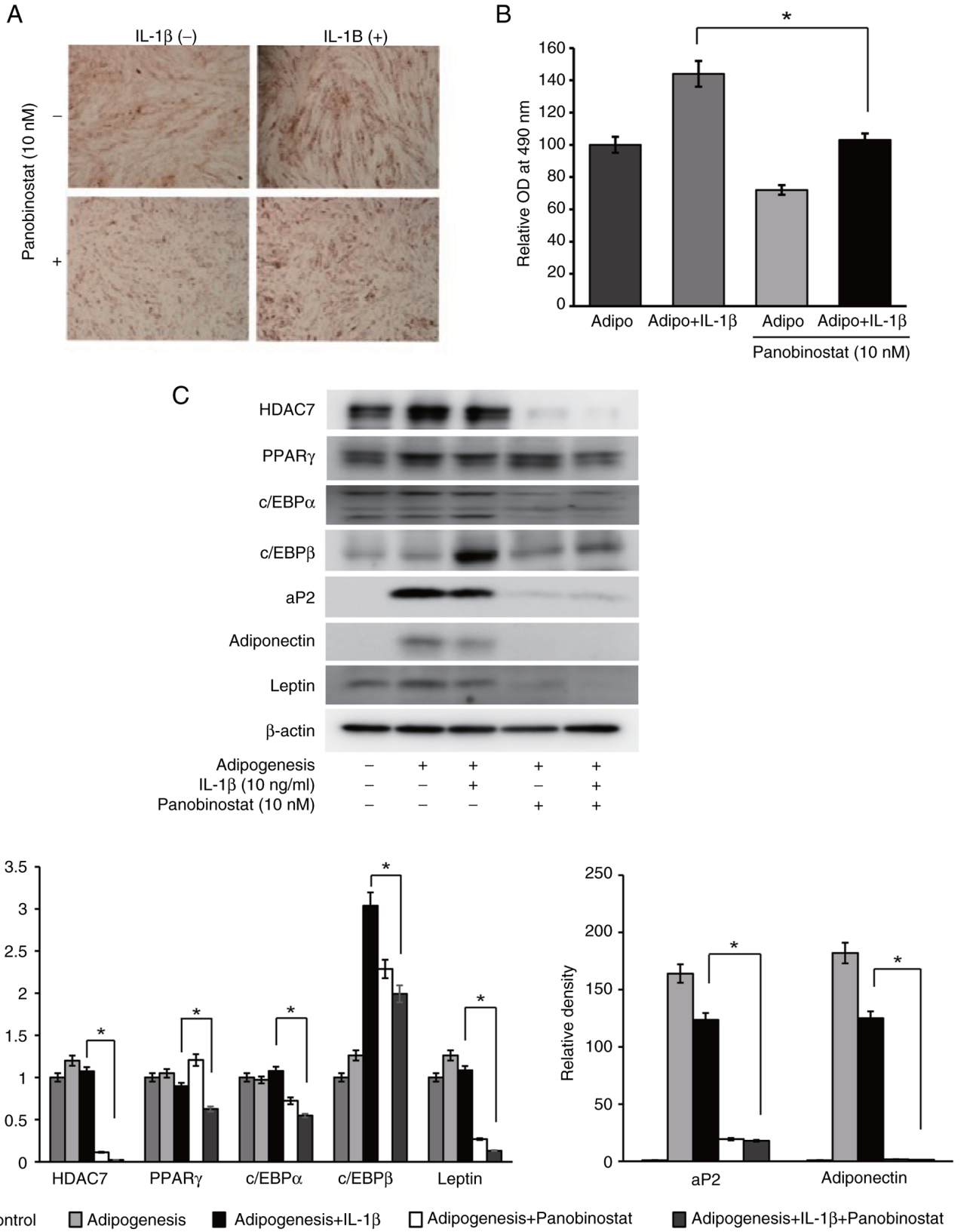

Figure 6. Suppressive effect of panobinostat on adipogenesis. Graves' orbitopathy orbital fibroblasts (n=3) were differentiated into adipocytes after 14 days of incubation in adipogenic medium. Panobinostat (10 nM) and/or IL-1β (10 ng/ml) was added during the adipogenesis. All experiments were performed twice. (A) To evaluate adipocyte differentiation, cells were stained with Oil Red O, and cytoplasmic lipid droplets were examined under a microscope (magnification, x40). (B) Stained cell lysates were solubilized, and absorbance was measured using a spectrophotometer at 490 nm. Data are presented as the mean ± SD. Statistical significance was determined using Mann-Whitney U-test to compare the effect of panobinostat under adipogenic stimulation with IL-1β. *P<0.05. (C) Adipogenic transcription factors, including PPARγ, c/EBPα, c/EBPβ, aP2, adiponectin and leptin, and HDAC7 were analyzed by western blotting after 14 days of adipogenic differentiation of orbital fibroblasts. Representative gel images are shown. (D) Densitometric analysis results of western blotting. Data are presented as the mean ± SD normalized to β-actin. Statistical significance was determined using Mann-Whitney U-test to compare the effect of panobinostat under adipogenic stimulation with IL-1β. *P<0.05. aP2, adipocyte protein 2; c/EBP, CCAAT-enhancer-binding protein; HDAC7, histone deacetylase 7; OD, optical density; PPARγ, peroxisome proliferator-activated receptor γ.

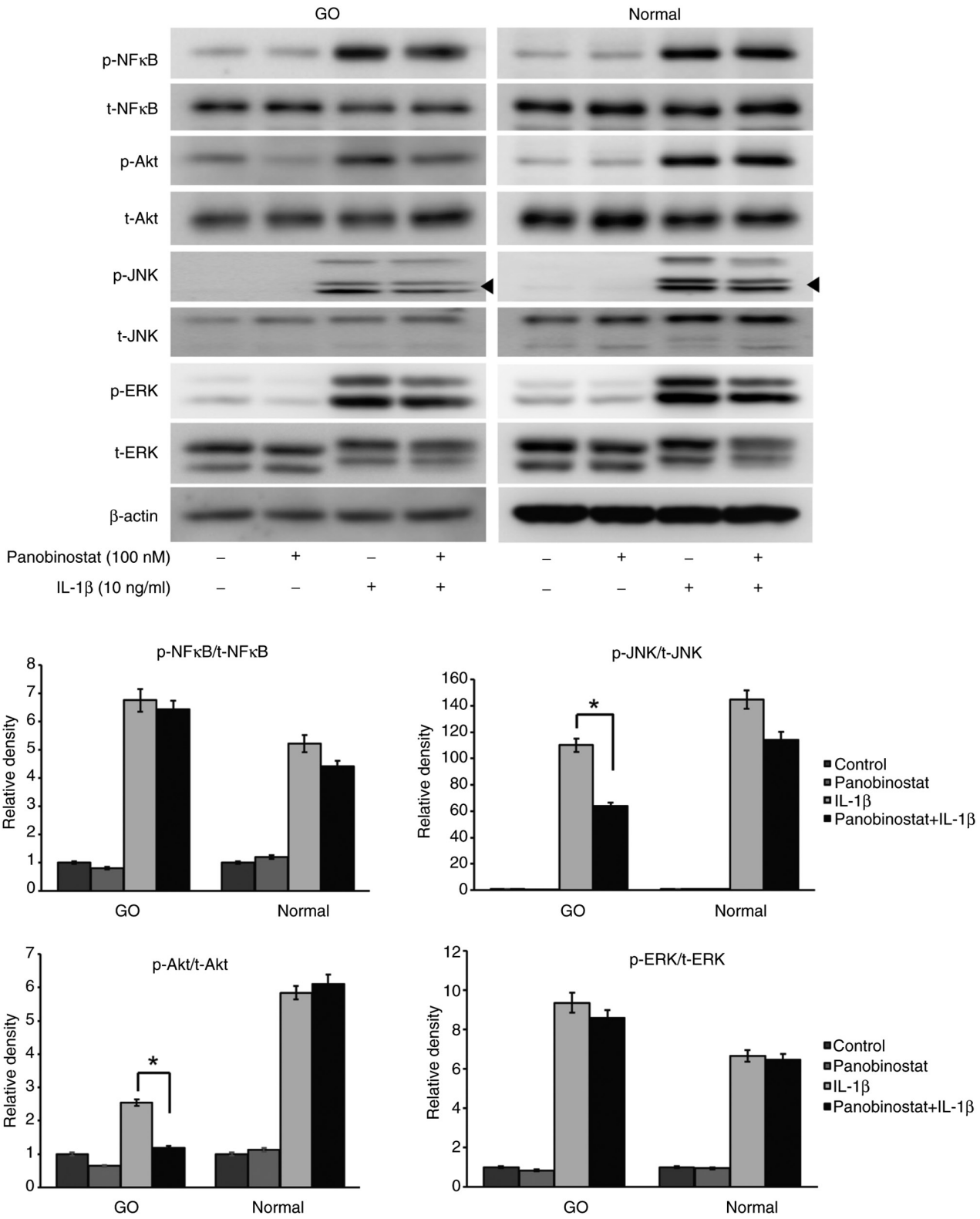

Figure 7. Effect of panobinostat on signal proteins under IL-1β stimulation. Orbital fibroblasts from patients with GO (n=3) and controls (n=3) were pretreated with panobinostat (100 nM) for 24 h, followed by IL-1β (10 ng/ml) treatment for 15 min. The t- and p-NF-κB, Akt, JNK and ERK proteins were analyzed through western blotting. Representative gel images are shown. Arrow indicates the p-JNK bands. β-actin was used as a loading control. After semi-quantification using densitometry, the ratio of p-/t-proteins was measured and compared with that of the control. Data are presented as the mean ± SD. Statistical significance was determined using Mann-Whitney U-test to compare the effect of panobinostat under IL-1β stimulation. *P<0.05. GO, Graves' orbitopathy; p-, phosphorylated; t-, total.

HDAC4 silencing reduced collagen 1α1, α-SMA, hyaluronan synthase 2 and hyaluronic acid production (22). This aligns with the present finding that HDAC inhibition could be a potential therapy for alleviating GO-related tissue remodeling. However, unlike previous research that focused on hyaluronan, the present study investigated proinflammatory cytokines,

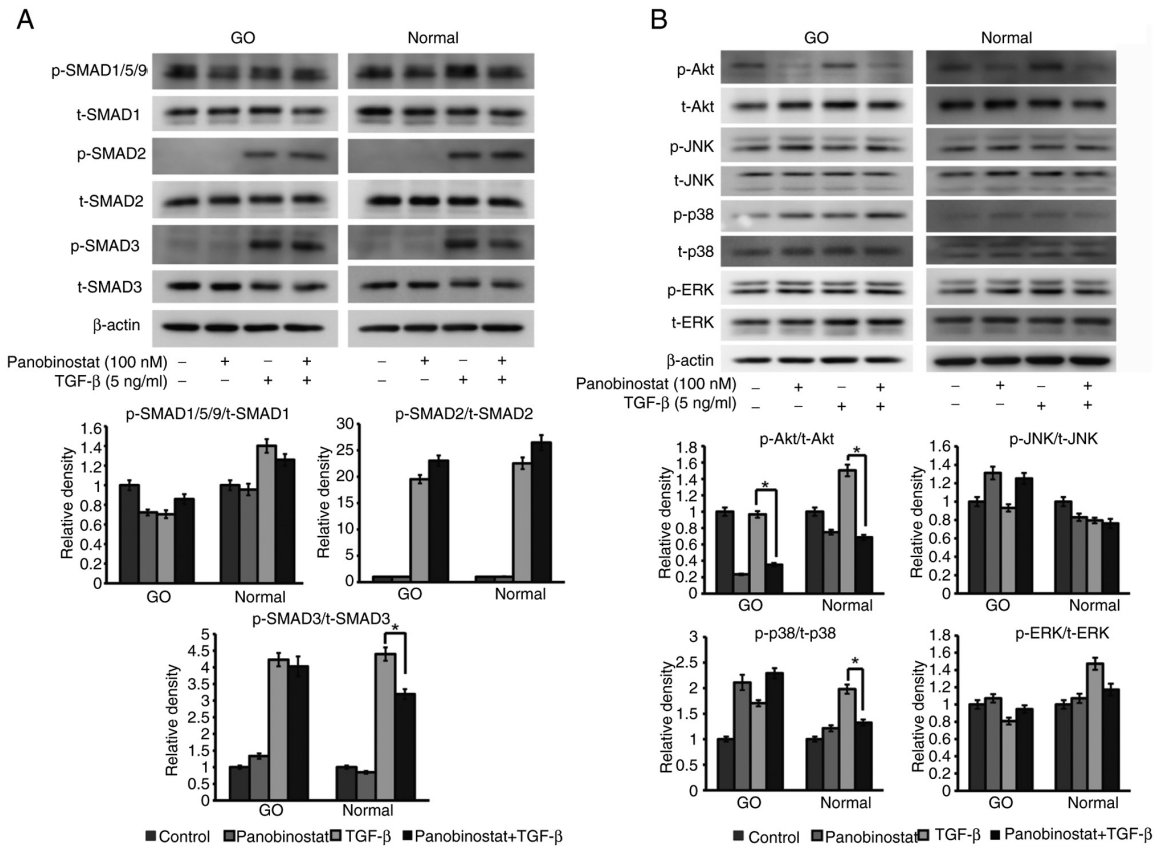

Figure 8. Effect of panobinostat on signal proteins under TGF-β stimulation. (A) Orbital fibroblasts were exposed to 100 nM panobinostat for 3 h, and then stimulated with TGF-β (5 ng/ml) for 1 h. The p-form of the SMAD signaling transducers, SMAD1/5/9, SMAD2 and SMAD3, were analyzed by western blotting, as were the total forms of SMAD1, SMAD2 and SMAD3. (B) Non-SMAD pathways under TGF-β (5 ng/ml) stimulation for 1 h were examined in orbital fibroblasts. Orbital fibroblasts were pretreated with 100 nM panobinostat for 3 h before TGF-β treatment. Western blot analysis of p- and t-Akt, JNK, p38 and ERK non-SMAD pathway molecules was performed. Orbital fibroblasts from three different GO samples and healthy subjects were used in the present study. β-actin was used as a loading control. The ratio of p-/t-proteins was measured and compared with that of the control, and data are presented as the mean ± SD. Statistical significance was determined using Mann-Whitney U-test to compare the effect of panobinostat under TGF-β stimulation. *P<0.05. GO, Graves' orbitopathy; p-, phosphorylated; t-, total.

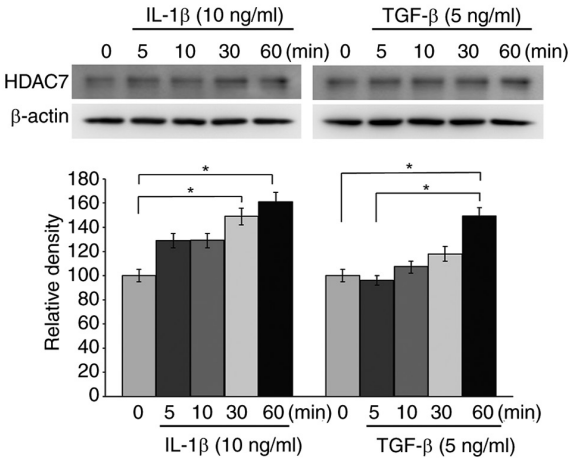

Figure 9. HDAC7 expression under stimulation with IL-1β and TGF-β in GO orbital fibroblasts. Orbital fibroblasts from patients with GO (n=3) were stimulated with IL-1β (10 ng/ml) and TGF-β (5 ng/ml) for increasing time intervals (0-60 min). HDAC7 release was measured at the indicated times (0, 5, 10, 30 and 60 min) through western blot analysis. Representative gel images are shown. β-actin was used as a loading control. All experiments were conducted twice on samples from 3 individuals. Data measured by densitometry are presented as the mean ± SD. Relative density was determined with respect to the 0-min time point. Each group was compared using the Kruskal-Wallis test followed by Dunn's post hoc test. *P<0.05. GO, Graves' orbitopathy; HDAC7, histone deacetylase 7.

which are the more fundamental causes of GO, including IL-6 and IL-8 (2,33-36). Another focus of the current study was fibrosis, which could potentially result in long-lasting impairment. Lastly, although PDGF-BB serves a pivotal role in GO pathogenesis, it stems from immune cells activated by numerous cytokines, including IL-1β, IFN-γ and TGF-β (37); therefore, Therefore, the inhibitory effects of panobinostat on broader regulators, such as IL-1β and TGF-β, which act upstream of PDGF-BB, may have a more significant impact on treating GO.

Despite their pan-inhibitory nature, the sensitivity of each pan-HDACi varies in different cellular contexts (28). In myeloma cells, panobinostat has been shown to predominantly upregulate HDAC6, uniquely reducing HDAC7 (38). In the present study, panobinostat exhibited a selective inhibitory effect on the mRNA expression levels of HDACs in GO orbital fibroblasts, reducing the expression of both HDAC6 and 7, while elevating HDAC3 expression. Similarly, another pan-HDACi, trichostatin A (TSA), has been reported to increase HDAC3 expression and decrease HDAC7 expression in the skin fibroblasts of patients with systemic sclerosis (39). The present study explored the therapeutic mechanism of panobinostat by targeting specific HDACs to mitigate the adverse effects associated with pan-HDAC inhibition. Specific inhibition

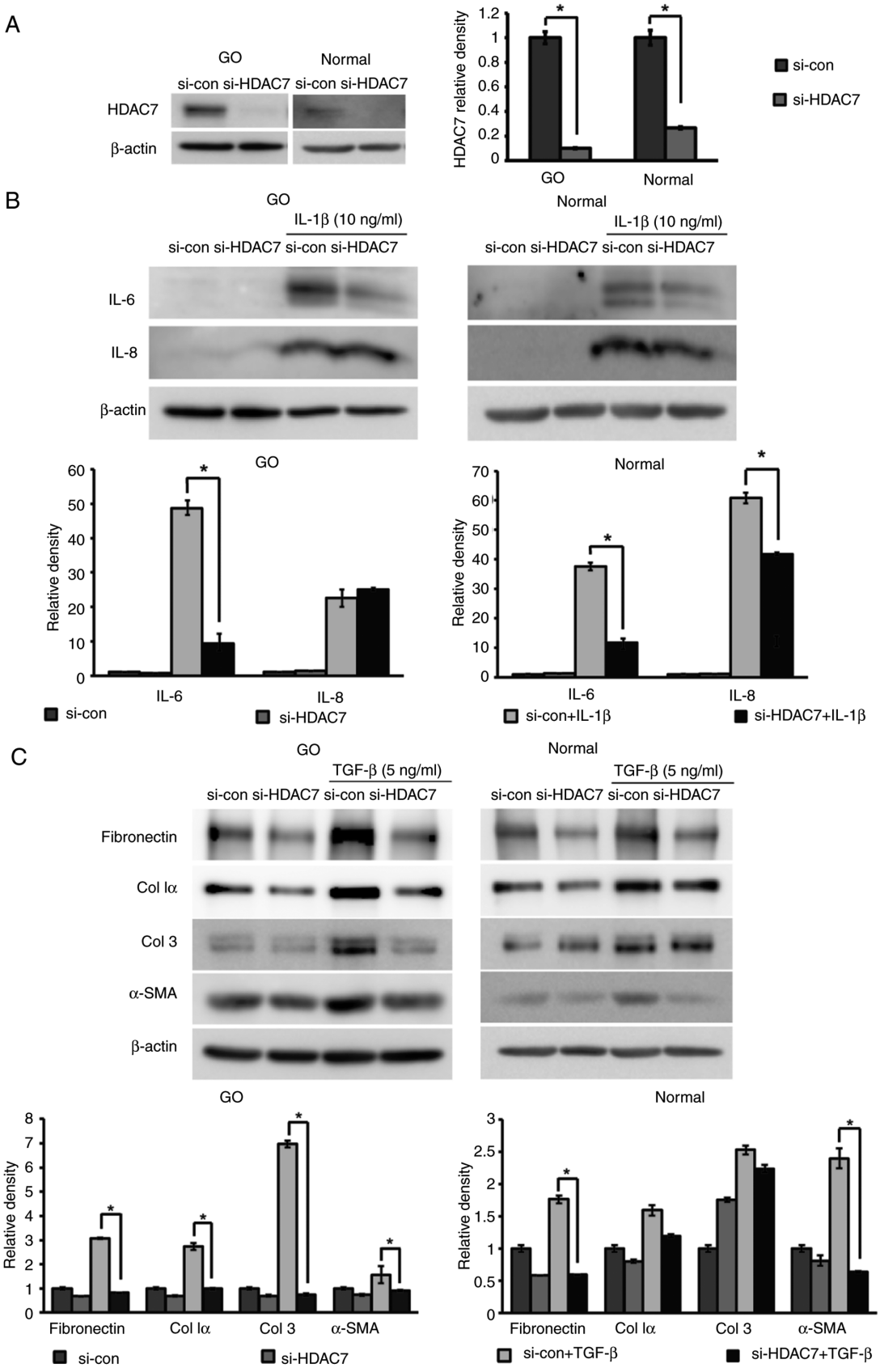

Figure 10. Anti-inflammatory and anti-fibrotic effects of silencing HDAC7 in orbital fibroblasts. HDAC7 was knocked down via transfection with siRNA (10 nM) for 24 h and cells were maintained for 48 h. (A) Silencing efficiency of si-HDAC7 was demonstrated in both GO and normal orbital fibroblasts (n=3) compared with si-con. (B) Cells were stimulated with IL-1β (10 ng/ml) for 24 h. Western blot analysis was performed to investigate the expression levels of the proinflammatory cytokines IL-6 and IL-8. (C) Orbital fibroblasts were treated with TGF-β (5 ng/ml) for 24 h, and profibrotic proteins, including fibronectin, Col Iα, Col 3 and α-SMA, were examined using western blot analysis. β-actin was used as a loading control for normalization. Each experiment was performed in duplicate. Data are presented as the mean ± SD. Statistical significance was determined using Mann-Whitney U-test to compare the effect of silencing HDAC7 under IL-1β or TGF-β stimulation. *P<0.05. α-SMA, α-smooth muscle actin; Col, collagen; con, control; GO, Graves' orbitopathy; HDAC7, histone deacetylase 7; si/siRNA, small interfering RNA.

using si-HDAC6 and si-HDAC7 confirmed that the downregulation of HDAC7 was associated with the anti-inflammatory and anti-fibrotic effects of panobinostat, in contrast to HDAC6 silencing, which showed no effect on the expression of inflammatory and fibrotic proteins. As the enzymatic activity of HDAC7 in the nucleus is influenced by HDAC3, which binds to silencing mediator of retinoic acid and thyroid hormone receptor and nuclear receptor corepressor (29), the present study examined whether the therapeutic effect of panobinostat could occur directly through HDAC7 reduction, not mediated by elevated HDAC3. Since HDAC7 reduction did not induce HDAC3 elevation, it was concluded that HDAC7 may independently mediate the therapeutic effect of panobinostat.

HDAC7 serves a crucial role in the pathogenesis of inflammation-related diseases associated with fibrosis. One study demonstrated that cytokine-induced type I collagen and fibronectin levels were reduced by TSA treatment through the inhibition of SMAD transcription factors in systemic sclerosis skin fibroblasts (40). In a subsequent study, it was confirmed that TGF-β-induced type I and type III collagen expression was reduced by HDAC7 knockdown (39). In fibroblasts derived from Peyronie's plaques, HDAC7 silencing has been shown to curtail fibroblast differentiation into myofibroblasts and decrease fibrotic protein production (41). In the lung tissue from a mouse model of ovalbumin-induced fibrosis, nuclear-translocated HDAC7 upon endothelin-1 stimulation promoted connective tissue growth factor production (42). Another study deemed HDAC7 pivotal for HDAC-dependent deacetylation in the promotor region of the anti-fibrotic gene PPARGC1A under TGF-β stimulation (19).

Previous studies have suggested that HDAC inhibition may affect the SMAD-dependent canonical TGF-β signaling pathway (40,41). However, the findings of the present study regarding the downstream target of panobinostat in orbital fibroblasts suggested that Akt was a possible signaling pathway molecule that may be present during both TGF-β and IL-1β stimulation. In a few previous studies on idiopathic pulmonary fibrosis, the PI3K-Akt signaling pathway was observed. Tubastatin A, a selective inhibitor of HDAC6, was shown to abrogate TGF-β-induced type I collagen expression by suppressing Akt phosphorylation in lung fibroblasts (43,44). Additionally, TSA treatment reduced α-SMA expression in response to TGF-β, which was dependent on HDAC4 mediated by phosphorylation of Akt (45). Taken together, Akt signaling may contribute to the therapeutic effects of HDAC inhibition not only on inflammation but also on GO fibrosis.

The present study has several limitations. First, the sample size for each experiment was limited and varied. The discrepancy in sample numbers arose due to differences in the invasiveness of collecting different types of samples, tissue or blood. To address the limitations associated with pooled sample analysis, subgroup analysis in patients with GO according to CAS was conducted in PBMCs, which did not reveal any significant differences (data not shown). Additionally, in the *in vitro* study using orbital fibroblasts, primary orbital fibroblasts were cultured from three different tissue samples in a randomized manner and the experiments were performed twice to obtain average results. This approach helped to minimize the limitations of pooled sample analysis by incorporating controlled variability and ensuring more representative results. Second, the experiments were limited to orbital fibroblasts. The present study is a preliminary *in vitro* study using orbital fibroblasts. Since a mouse model for GO is currently under investigation and shows promising results (46), HDACis could potentially be applied to *in vivo* systems. Lastly, unlike pan-HDACis, a specific HDACi could be used. Using a specific HDACi is desirable to reduce the effects on other HDACs and to minimize the toxicity associated with pan-HDAC inhibition. To date, only a few potent HDAC7is have been identified. They exhibit high potency as HDAC7is; however, they also affect other class IIa HDACs (HDAC4, 5 and 9) (47). Notably, class IIa HDACs are associated with various immune cells, including macrophages and lymphocytes (48). Furthermore, given that HDAC4, one of the class IIa HDACs, has been recognized as a target for hyaluronan production in GO (22), HDAC7is still have therapeutic potential against GO even though they inhibit other class IIa HDACs in addition to HDAC7. Further investigation is necessary when considering the use of HDAC7is *in vivo*.

In conclusion, the present study on GO highlights the therapeutic potential of HDAC inhibition. Specifically, panobinostat was identified as a potent inhibitor of proinflammatory, adipogenic and profibrotic stimulation in GO orbital fibroblasts, predominantly via the Akt signaling pathway. The anti-inflammatory and anti-fibrotic actions of panobinostat were evident through its downregulation of HDAC7 mRNA expression. Considering the crucial role of HDACs in autoimmune processes and fibrosis, the present findings demonstrate the potential of HDAC7-targeted interventions. As the understanding of GO pathogenesis advances, the current study proposes epigenetic modulation, especially by targeting HDAC7, as a promising therapeutic option. Further studies should focus on elucidating broader molecular mechanisms and validating these findings *in vivo*.

Acknowledgements

Portions of this study were presented at the ASOPRS 2022 Fall Scientific Symposium (Chicago, IL, USA).

Funding

This work was supported by the National Research Foundation of Korea grant funded by the Korean government (Ministry of Science and ICT; grant no. RS-2023-00208570).

Availability of data and materials

The data generated in the present study may be requested from the corresponding author.

Authors' contributions

JSY and HJB designed the present study. SHC performed the experiments, and JSY, HJB and JK confirmed the authenticity of all the raw data. JSY, HJB, JK and DOK analyzed and interpreted the data. JSY and JK provided the laboratory, reagents and materials, and JK procured the funding. HJB, SHC and DOK wrote the manuscript, and JSY and JK edited it. All authors have read and approved the final version of the manuscript.

Ethics approval and consent to participate

The present study was conducted according to the guidelines of The Declaration of Helsinki, and was approved by the Institutional Review Board of the Severance Hospital, Yonsei University College of Medicine (IRB no. 4-2022-0244; Seoul, South Korea). Written informed consent was obtained from all subjects involved in the study.

Patient consent for publication

Not applicable.

Competing interests

The authors declare that they have no competing interests.

References

1. Lazarus JH: Epidemiology of Graves' orbitopathy (GO) and relationship with thyroid disease. Best Pract Res Clin Endocrinol Metab 26: 273-279, 2012.
2. Bahn RS: Graves' ophthalmopathy. N Engl J Med 362: 726-738, 2010.
3. Bartley GB, Fatourechi V, Kadrmas EF, Jacobsen SJ, Ilstrup DM, Garrity JA and Gorman CA: Clinical features of Graves' ophthalmopathy in an incidence cohort. Am J Ophthalmol 121: 284-290, 1996.
4. Rotondo Dottore G, Torregrossa L, Lanzolla G, Mariotti S, Menconi F, Piaggi P, Cristofani Mencacci L, Posarelli C, Maglionico MN, Dallan I, *et al*: Role of the mononuclear cell infiltrate in Graves' orbitopathy (GO): Results of a large cohort study. J Endocrinol Invest 45: 563-572, 2022.
5. Huang Y, Fang S, Li D, Zhou H, Li B and Fan X: The involvement of T cell pathogenesis in thyroid-associated ophthalmopathy. Eye (Lond) 33: 176-182, 2019.
6. Yin X, Latif R, Bahn R and Davies TF: Genetic profiling in Graves' disease: Further evidence for lack of a distinct genetic contribution to Graves' ophthalmopathy. Thyroid 22: 730-736, 2012.
7. Hadj-Kacem H, Rebuffat S, Mnif-Féki M, Belguith-Maalej S, Ayadi H and Péraldi-Roux S: Autoimmune thyroid diseases: Genetic susceptibility of thyroid-specific genes and thyroid autoantigens contributions. Int J Immunogenet 36: 85-96, 2009.
8. Wang Y, Ma XM, Wang X, Sun X, Wang LJ, Li XQ, Liu XY and Yu HS: Emerging insights into the role of epigenetics and gut microbiome in the pathogenesis of Graves' ophthalmopathy. Front Endocrinol (Lausanne) 12: 788535, 2022.
9. Rotondo Dottore G, Bucci I, Lanzolla G, Lanzolla G, Dallan I, Sframeli A, Torregrossa L, Casini G, Basolo F, Figus M, *et al*: Genetic profiling of orbital fibroblasts from patients with Graves' orbitopathy. J Clin Endocrinol Metab 106: e2176-e2190, 2021.
10. Kouzarides T: Chromatin modifications and their function. Cell 128: 693-705, 2007.
11. Shakespear MR, Halili MA, Irvine KM, Fairlie DP and Sweet MJ: Histone deacetylases as regulators of inflammation and immunity. Trends Immunol 32: 335-343, 2011.
12. Narita T, Weinert BT and Choudhary C: Functions and mechanisms of non-histone protein acetylation. Nat Rev Mol Cell Biol 20: 156-174, 2019.
13. Gatla HR, Muniraj N, Thevkar P, Yavvari S, Sukhavasi S and Makena MR: Regulation of chemokines and cytokines by histone deacetylases and an update on histone decetylase inhibitors in human diseases. Int J Mol Sci 20: 1110, 2019.
14. Chen H, Pan J, Wang JD, Liao QM and Xia XR: Suberoylanilide hydroxamic acid, an inhibitor of histone deacetylase, induces apoptosis in rheumatoid arthritis fibroblast-like synoviocytes. Inflammation 39: 39-46, 2016.
15. Bahn RS: Thyrotropin receptor expression in orbital adipose/connective tissues from patients with thyroid-associated ophthalmopathy. Thyroid 12: 193-195, 2002.
16. Zhang Y and Zhang B: Trichostatin A, an inhibitor of histone deacetylase, inhibits the viability and invasiveness of hypoxic rheumatoid arthritis fibroblast-like synoviocytes via PI3K/Akt signaling. J Biochem Mol Toxicol 30: 163-169, 2016.
17. Oh BR, Suh DH, Bae D, Ha N, Choi YI, Yoo HJ, Park JK, Lee EY, Lee EB and Song YW: Therapeutic effect of a novel histone deacetylase 6 inhibitor, CKD-L, on collagen-induced arthritis in vivo and regulatory T cells in rheumatoid arthritis in vitro. Arthritis Res Ther 19: 154, 2017.
18. de Zoeten EF, Wang L, Butler K, Beier UH, Akimova T, Sai H, Bradner JE, Mazitschek R, Kozikowski AP, Matthias P and Hancock WW: Histone deacetylase 6 and heat shock protein 90 control the functions of Foxp3(+) T-regulatory cells. Mol Cell Biol 31: 2066-2078, 2011.
19. Jones DL, Haak AJ, Caporarello N, Choi KM, Ye Z, Yan H, Varelas X, Ordog T, Ligresti G and Tschumperlin DJ: TGFβ-induced fibroblast activation requires persistent and targeted HDAC-mediated gene repression. J Cell Sci 132: jcs233486, 2019.
20. Korfei M, Stelmaszek D, MacKenzie B, Skwarna S, Chillappagari S, Bach AC, Ruppert C, Saito S, Mahavadi P, Klepetko W, *et al*: Comparison of the antifibrotic effects of the pan-histone deacetylase-inhibitor panobinostat versus the IPF-drug pirfenidone in fibroblasts from patients with idiopathic pulmonary fibrosis. PLoS One 13: e0207915, 2018.
21. Sanders YY, Hagood JS, Liu H, Zhang W, Ambalavanan N and Thannickal VJ: Histone deacetylase inhibition promotes fibroblast apoptosis and ameliorates pulmonary fibrosis in mice. Eur Respir J 43: 1448-1458, 2014.
22. Ekronarongchai S, Palaga T, Saonanon P, Pruksakorn V, Hirankarn N, van Hagen PM, Dik WA and Virakul S: Histone deacetylase 4 controls extracellular matrix production in orbital fibroblasts from graves' ophthalmopathy patients. Thyroid 31: 1566-1576, 2021.
23. Atadja P: Development of the pan-DAC inhibitor panobinostat (LBH589): Successes and challenges. Cancer Lett 280: 233-241, 2009.
24. Shao W, Growney J, Feng Y, Wang P, Yan-Neale Y, O'Connor G, Kwon P, Yao YM Fawell S and Atadja P: Potent anticancer activity of a pan-deacetylase inhibitor panobinostat (LBH589) as a single agent in in vitro and in vivo tumor models. Cancer Res 68 (9 Suppl): S735, 2008.
25. Mourits MP, Koornneef L, Wiersinga WM, Prummel MF, Berghout A and van der Gaag R: Clinical criteria for the assessment of disease activity in Graves' ophthalmopathy: A novel approach. Br J Ophthalmol 73: 639-644, 1989.
26. Livak KJ and Schmittgen TD: Analysis of relative gene expression data using real-time quantitative PCR and the 2(-Delta Delta C(T)) method. Methods 25: 402-408, 2001.
27. Byeon HJ, Chae MK, Ko J, Lee EJ, Kikkawa DO, Jang SY and Yoon JS: The role of adipsin, complement factor D, in the pathogenesis of Graves' orbitopathy. Invest Ophthalmol Vis Sci 64: 13, 2023.
28. Dokmanovic M, Perez G, Xu W, Ngo L, Clarke C, Parmigiani RB and Marks PA: Histone deacetylase inhibitors selectively suppress expression of HDAC7. Mol Cancer Ther 6: 2525-2534, 2007.
29. Fischle W, Dequiedt F, Fillion M, Hendzel MJ, Voelter W and Verdin E: Human HDAC7 histone deacetylase activity is associated with HDAC3 in vivo. J Biol Chem 276: 35826-35835, 2001.
30. Yan N, Zhou JZ, Zhang JA, Cai T, Zhang W, Wang Y, Muhali FS, Guan L and Song RH: Histone hypoacetylation and increased histone deacetylases in peripheral blood mononuclear cells from patients with Graves' disease. Mol Cell Endocrinol 414: 143-147, 2015.
31. Tan C, Xuan L, Cao S, Yu G, Hou Q and Wang H: Decreased histone deacetylase 2 (HDAC2) in peripheral blood monocytes (PBMCs) of COPD patients. PLoS One 11: e0147380, 2016.
32. Li Y, Zhou M, Lv X, Song L, Zhang D, He Y, Wang M, Zhao X, Yuan X, Shi G and Wang D: Reduced activity of HDAC3 and increased acetylation of histones H3 in peripheral blood mononuclear cells of patients with rheumatoid arthritis. J Immunol Res 2018: 7313515, 2018.
33. Xie K: Interleukin-8 and human cancer biology. Cytokine Growth Factor Rev 12: 375-391, 2001.
34. Sampson AP: The role of eosinophils and neutrophils in inflammation. Clin Exp Allergy 30 (Suppl 1): S22-S27, 2000.
35. Gu LQ, Jia HY, Zhao YJ, Liu N, Wang S, Cui B and Ning G: Association studies of interleukin-8 gene in Graves' disease and Graves' ophthalmopathy. Endocrine 36: 452-456, 2009.
36. Antonelli A, Fallahi P, Elia G, Ragusa F, Paparo SR, Ruffilli I, Patrizio A, Gonnella D, Giusti C, Virili C, *et al*: Graves' disease: Clinical manifestations, immune pathogenesis (cytokines and chemokines) and therapy. Best Pract Res Clin Endocrinol Metab 34: 101388, 2020.
37. Virakul S, van Steensel L, Dalm VASH, Paridaens D, van Hagen PM and Dik WA: Platelet-derived growth factor: A key factor in the pathogenesis of graves' ophthalmopathy and potential target for treatment. Eur Thyroid J 3: 217-226, 2014.

38. Cheng T, Kiser K, Grasse L, Iles L, Bartholomeusz G, Samaniego F, Orlowski RZ and Chandra J: Expression of histone deacetylase (HDAC) family members in bortezomib-refractory multiple myeloma and modulation by panobinostat. Cancer Drug Resist 4: 888-902, 2021.
39. Hemmatazad H, Rodrigues HM, Maurer B, Brentano F, Pileckyte M, Distler JH, Gay RE, Michel BA, Gay S, Huber LC, *et al*: Histone deacetylase 7, a potential target for the antifibrotic treatment of systemic sclerosis. Arthritis Rheum 60: 1519-1529, 2009.
40. Huber LC, Distler JHW, Moritz F, Hemmatazad H, Hauser T, Michel BA, Gay RE, Matucci-Cerinic M, Gay S, Distler O and Jüngel A: Trichostatin A prevents the accumulation of extracellular matrix in a mouse model of bleomycin-induced skin fibrosis. Arthritis Rheum 56: 2755-2764, 2007.
41. Kang DH, Yin GN, Choi MJ, Song KM, Ghatak K, Minh NN, Kwon MH, Seong DH, Ryu JK and Suh JK: Silencing histone deacetylase 7 alleviates transforming growth factor-β1-induced profibrotic responses in fibroblasts derived from peyronie's plaque. World J Mens Health 36: 139-146, 2018.
42. Hua HS, Wen HC, Weng CM, Lee HS, Chen BC and Lin CH: Histone deacetylase 7 mediates endothelin-1-induced connective tissue growth factor expression in human lung fibroblasts through p300 and activator protein-1 activation. J Biomed Sci 28: 38, 2021.
43. Saito S, Zhuang Y, Shan B, Danchuk S, Luo F, Korfei M, Guenther A and Lasky JA: Tubastatin ameliorates pulmonary fibrosis by targeting the TGFβ-PI3K-Akt pathway. PLoS One 12: e0186615, 2017.
44. Liu Y, Wang R, Han H and Li L: Tubastatin A suppresses the proliferation of fibroblasts in epidural fibrosis through phosphatidylinositol-3-kinase/protein kinase B/mammalian target of rapamycin (PI3K/AKT/mTOR) signalling pathway. J Pharm Pharmacol 74: 426-434, 2022.
45. Guo W, Shan B, Klingsberg RC, Qin X and Lasky JA: Abrogation of TGF-beta1-induced fibroblast-myofibroblast differentiation by histone deacetylase inhibition. Am J Physiol Lung Cell Mol Physiol 297: L864-L870, 2009.
46. Bao Y, Kim D, Cho YH, Ku CR, Yoon JS and Lee EJ: Cre-loxP system-based mouse model for investigating Graves' disease and associated orbitopathy. Thyroid 33: 1358-1367, 2023.
47. Wang Y, Abrol R, Mak JYW, Das Gupta K, Ramnath D, Karunakaran D, Fairlie DP and Sweet MJ: Histone deacetylase 7: A signalling hub controlling development, inflammation, metabolism and disease. FEBS J 290: 2805-2832, 2023.
48. Liu L, Dong L, Bourguet E and Fairlie DP: Targeting class IIa HDACs: Insights from phenotypes and inhibitors. Curr Med Chem 28: 8628-8672, 2021.